SEMARAK ILMU
PUBLISHING

Journal of Advanced Research in Applied Sciences and Engineering Technology

Journal homepage:
https://semarakilmu.com.my/journals/index.php/applied_sciences_eng_tech/index
ISSN: 2462-1943

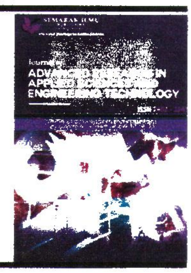

Blast Impulse Variations in the NATO STANAG 4569 Testing Procedures for Armoured Vehicle Protection Level Evaluation.

Zulkifli Abu Hassan*, Aniza Ibrahim, Noor Aina Misnon, Vikneswaran Munikanan, Muhammad Syahmi Abd. Malek & Muhamad Ikhmal Rusli

Department of Civil Engineering, Faculty of Engineering, National Defence University of Malaysia, 57000 Sg Besi, Kuala Lumpur, Malaysia

ARTICLE INFO

Article history:
Received
Received in revised form
Accepted
Available online

Keywords:
STANAG 4569; buried explosive; small-scale experiment; vehicle protective system; blast energy transfer

ABSTRACT

The standard used in NATO countries for armoured vehicle protection level evaluation is the STANAG 4569 AEP-55. There are two options for test conditions described in the procedure. Both test conditions are equally accepted to be used in assessing the compliance of the vehicle mine protection requirements. A test condition that applies surrogate mine in a steel pot test condition requires less complicated preparation, which is opted for by many compared to the buried setup. However, characteristics of blast output from buried in-soil test setup would possibly alter the blast loading to the vehicle's undercarriage. There could be significant variations in blast intensity and other effects in both test setups. This study conducted a small-scale experimental test to measure the effects of global and localise impact caused by a buried explosive in Sandy Gravel and Steel Pot test conditions. Results showed global average energy transfer and average global peak acceleration in Sandy gravel test condition are respectively 40 % and 21 % higher than in Steel Pot. The localised effect showed that residual deformation is higher by 5% in Steel Pot compared to Sandy Gravel tests. However, average peak deformation and average local peak acceleration in Sandy gravel are 8% higher compared to Steel pot.

1. Introduction

The new generation of high mobility armoured vehicles (HMAV) adopted international testing standards to certify their products' protective system's reliability. One of them is the NATO STANAG 4569. The STANAG 4569 and AEP-55 for armoured vehicle protection level evaluation is the standard used in NATO countries. It is used to verify the integrity and deployability of armoured vehicles from member countries. This also indicates that the vehicle, regardless of its make and country of origin, meets the standardised level and is safe against specific threats outlined by the standards. Many other countries, including Malaysia [1], have embraced the STANAG 4569 procedures, specifically for protection against blast mine threats (Level 2-4).

* *Corresponding author.*
E-mail address: zulabha@upnm.edu.my

https://doi.org/10.37934/araset.XX.X.XX

There are two possible options for test conditions described in the procedure: i) detonation of surrogate mine buried in water-saturated sandy gravel (Sandy Gravel), and ii) detonation of surrogate mine in a steel pot (Steel Pot)[2]. These testing conditions are accepted in certifying the vehicle's integrity against landmine blasts. Member countries may conduct tests based on the described test conditions to confirm their vehicles' compliance with the STANAG 4569-AEP55 requirements. For the landmine blast in the steel pot, an explosive charge is detonated in a steel block hollow recess with a standard diameter and depth. Unlike steel pot testing conditions, the landmine blast in the saturated sandy gravel, the explosive charge is detonated in the sandy gravel pit where it is buried shallowly at a specific depth. It involves the preparation of a large sandy gravel pit and requires a specific gravel size and distribution [3]. However, the steel pot testing condition has higher repeatability [4], and the simplicity of the testing preparation makes it more common over sandy gravel testing conditions.

Nevertheless, the nature of the test conditions is different. While the geotechnical properties of the soil have no influence on detonation in the steel pot, the detonation in sandy gravel may be affected by the soil's effects, such as from the ejecta impact and funnelling blast load from the crater [5] [6]. Consequently, there are significant variations in the magnitude of blast loads imparted from these two test conditions. This situation results in the amount of energy transferred or the impact being superior in one of the test conditions. Although STANAG recognises the existence of loading variations in testing in soil, it is still up to the National Authority of the member countries to decide on which testing condition should be adopted based on their requirements.

Particularly in the defence industries, the standards have been widely accepted as a benchmark in many countries. Companies or manufacturers of armoured vehicles have often quoted in their claim that they offer STANAG 4569-certified armoured vehicles. In other words, provide levels of protection in compliance with the STANAG 4569-AEP55 requirements. Though the claim might be credible, results from the tests may not represent the actual safety evaluation and assessment since it was not mentioned or known to which approach of test conditions was implemented. Discrepancies can be determined by comparing effect variations between the two testing conditions, and a corrective coefficient would supplement data required for improving protective structure design capability and normalising test results from both testing conditions in anticipating optimum safety compliance.

Experimental blast tests using a small-scale test apparatus and explosive charge [7] [8] were carried out in this study to determine the blast effects in terms of energy transfer to the test apparatus and its peak acceleration and acceleration of the target plate and its peak and residual deformations. This paper presents the findings on blast impact variations of global and local effects based on the observation of the response of the above-ground test apparatus. The outcome of the explosive detonation is intended to simulate the two test conditions described in STANAG 4569 AEP55.

2. Shallow Buried Detonation in Soils

Experimental works have been carried out to investigate how soil geotechnical properties affect blast output. In the testbed of remoulded soil, tests were performed by simulating the detonation of buried explosives. The properties and conditions of the soil have been observed and found to have a substantial impact on the quantity and severity of blast loads. In terms of blast output characteristics, studies on soil types such as Leighton Buzzard sands, Red Building sand, concrete fine aggregate sand (CFAS), fine-grained Prairie soil, and Brown Laminated Silty Clay have demonstrated unique behaviour [9] [10]. The intensity of a landmine explosion was reported to be influenced by soil properties, including moisture content, particle size distribution, and density. Other factors, such as the depth of burial (DOB) [11] and explosive charge size, also contributed to the variations in blast intensity. The strength of the blast load can be influenced by each of these factors separately, but they are always connected.

According to Ehrgott *et al.,* [12], on the impact of soil particle size on imparted blast impulse, explosive charges buried in fine-grained soils explode more powerfully than those buried in coarse-grained soils. According to the experimental findings, the peak total impulses in clayey soil are 40% higher than those in silty sand and 60% higher than those in sandy soil when buried charges are detonated. Additionally, it was discovered that while having equal moisture contents, different soil types with varied particle size distributions exhibit diversity in blast intensity.

In the experiment reproduced in silty-clay, fine-grained Suffield Prairie soil and coarse-grained concrete fine aggregate sand (CFAS) [9], a 20% moisture content increment in both materials was observed in the ability of Prairie soil to transfer energy seven times more effectively than a detonation in CFAS. Prairie soil has additionally shown that a 20% increase in moisture content might boost the blast energy, reaching a target by five times greater compared to a detonation on dry Prairie soil. When it comes to the sandy gravel scenario described in AEP-55, the sandy gravel soil in its saturated condition produces a stronger impulse than finer soil with less water. However, finer soil with more water content generates higher impulses than sandy gravel soil, which is a completely saturated [5].

It was also claimed that the way the blast-load concentration is propelled upward was affected by soil characteristics associated with grain size. Detonation products and ejecta mass momentum are both present in the blast load concentration [13] [14]. The form and creation of craters show that the explosion load was concentrated and redirected. It is influenced by soil characteristics as well as the depth at which the explosive is buried [15] [16]. However, Rigby *et al.,* [17] discovered that the soil's particle size and cohesiveness or lack thereof have no appreciable impact on the loading process. A region above the charge receives more localised particle hits from well-graded and stiffer soil. This is evident in well-graded sandy gravel soil, which demonstrates a more concentrated loading distribution despite imparting a smaller impulse [5].

Bergeron *et al.,* [15] explained detonation phases in soil, which include the gas expansion phase and the ejecta phase. Different types of soil with different properties characterize each phase differently, which contributes to the unique shape of the crater, the funnelling effect of the blast load and impacting ejecta [6]. Detonation of shallowly buried explosives in residual soil is 4 times higher than detonation in silica sand, and the impacting impulse created in detonation in silica sand is almost 5 times greater than detonation above ground [18]. For a detonation of the explosive charge that does not create cratering effects, it is anticipated that the characteristics of a blast load may exhibit similar effects of blast above the ground surface as it affects the geometry of the explosion.

3. STANAG 4569-AEP55 Testing Conditions

STANAG 4569 and AEP 55 are NATO standards used to assess the protection level of military vehicles against ballistic threats and mine explosions, respectively. STANAG 4569 outlines the levels of protection against gunfire, artillery fragments, and other similar threats, while AEP 55 focuses on the vehicle's ability to withstand explosions from landmines and IEDs. These standards help ensure that military vehicles meet specific safety requirements and can effectively protect their occupants in various combat situations.

In the context of AEP-55 certification for military vehicles' resistance to mine and IED blasts, "Steel Pot" and "Sandy Gravel" are two different testing conditions that simulate specific types of terrains and explosive threats. These different testing conditions help evaluate how well a military vehicle can withstand explosions in various real-world scenarios, taking into account the characteristics of different terrains and their interaction with explosive forces. The goal is to ensure that the vehicle's design provides adequate protection to its occupants and maintains its operational capabilities under different blast conditions. The reference test setup for the two testing conditions is shown in Figure 1.

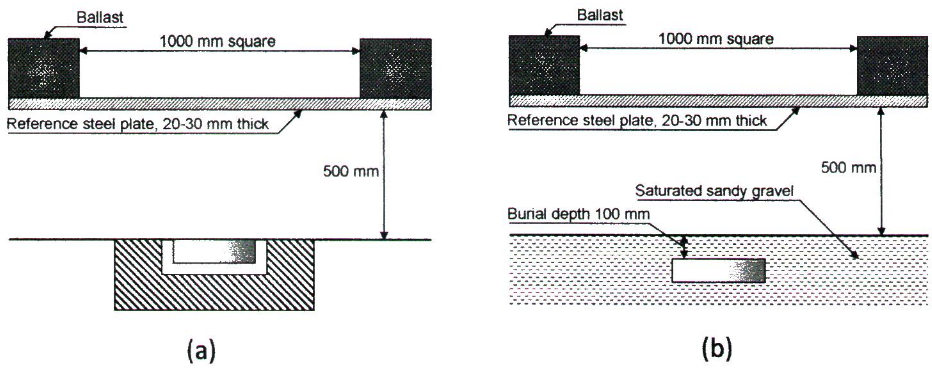

Fig. 1. Reference test-setup for mine in (a) steel pot (b) sandy gravel [2]

Steel Pot testing condition is designed to simulate a blast event occurring on a hard, rigid surface, similar to the detonation of an explosive device on a paved road or a concrete surface. It represents scenarios where the shockwave generated by the explosion is efficiently transmitted through a solid medium, potentially causing greater structural damage to the vehicle.

Sandy Gravel testing condition simulates a blast event occurring on a natural ground condition, such as a sandy or gravelly road. The granular nature of the terrain can absorb and dissipate some of the shockwave energy, potentially resulting in different effects on the vehicle's structure and occupants compared to the Steel Pot condition.

Steel Pot testing condition, however, provides easier-to-control and reproducible test conditions [2]. While the Sandy Gravel testing condition, the test bed is filled up with soil particles with sizes ranging from 0.08 mm to 40 mm, which is a well-graded particle size distribution. Unlike Steel Pot, sandy gravel with such particle size distribution suggested less repeatable test results [4].

4. Experimental Procedure

The method adopted for the study is a Free Acceleration Approach (FAA) method [19] [20] [21] [22]. In this method, the apparatus is not restrained, and its motion is not controlled by any mechanical guide. It is free to move upwards and the deceleration of the apparatus depends only on gravity.

4.1 Small Scale Test Apparatus

The test equipment used in this experimental study is similar to the previous work by Hassan *et al.,* [7](Figure 2). The test apparatus is made to be portable, simple to set up at test locations, and usable more than once. It is scaled at 1/10th (scale factor 10) to approximate the size and weight of an armoured vehicle. The test apparatus consists of a steel test jig, a deformation-gauge box, and a steel target plate.

The test jig's primary frame is composed of four C-section mild steel sections to create a square frame that measures 500 mm x 500 mm and leaves a square opening measuring 390 on each side. For plastic impact, a sacrificial replaceable steel plate was utilised as the target plate. The target plate with a dimension of 500 mm x 500 mm x 5 mm thickness is bolted at the bottom side of the frame.

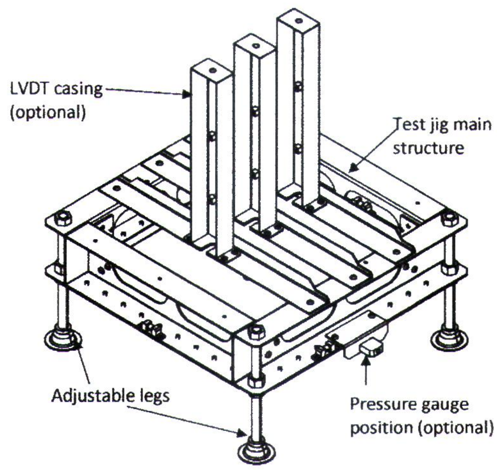

Fig. 2. Test apparatus [7]

A deformation-gauge box containing synthetic clay is used to measure the peak deflection of the target plate, which is fixed at the top frame's struts (Figure 3) Adjustable steel legs secured to the four corners of the steel frame support the test jig. This enables changes to determine the necessary stand-off distance between the target plate's face and the ground. The apparatus's total weight, including the steel jig, steel plate, and deformation-gauge box, was around 24 kg.

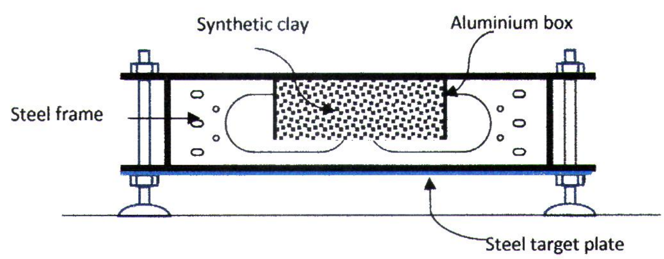

Fig. 3. Cross-section of the test apparatus

In this experiment, a 20 g mass of high explosive ammonium nitrate (AN) emulsion explosive charge (Emulex) was used to conduct each blast test. The charge assembly is depicted in Figure 4. Heavy-duty paper casing with a height-to-diameter (H/D) ratio of roughly 0.33 was used to mould the explosive charge into a disc-shaped charge [2]. The disc-shaped charge was placed with a detonator that had a secondary charge mass of 720 mg pentaerythritol tetranitrate (PETN), about half the depth of the charge.

4.2 Test Setup

The blast tests were carried out in two test conditions: buried in a Sandy Gravel bed (SG Test) and in the Steel Pot (SP Test). For the Sandy Gravel test condition, the soil used has a uniform particle size distribution between 1 mm to 4.75 mm with uniformity coefficient (C_u) and coefficient of gradation (C_c) of 1.9 and 0.9, respectively. The sandy gravel testbed was prepared by depositing the moist soil into a 0.55 x 0.55 x 0.30 m pit box in the ground with a compacted soil density of about 1631 kg/m^3 (Figure 5).

The explosive charge was buried in the testbed aligned to the target plate's centre. Figure 6 shows the setup in the Sandy Gravel Test condition. The depth from the ground surface to the top surface of the explosive was specified at 10 mm, and this distance is defined as the depth of burial (DOB).

Fig. 5. Sandy Gravel is deposited into the pit box up to the ground level

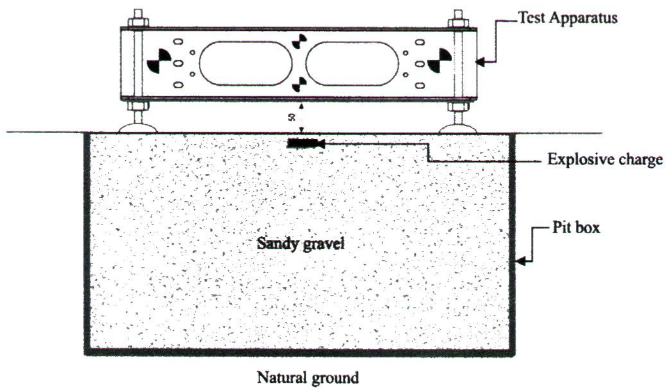

Fig. 6. Setup for Sandy Gravel testing condition

The Steel Pot test was prepared by placing the steel pot at the ground surface level, and the explosive charge was placed in the recessed circle of the steel pot (Figure 7). Figure 8 shows the setup in the Steel Pot test condition. In both test setups, the test apparatus was positioned upright on the ground, and its height relative to the target plate was adjusted to a predetermined height by adjustable legs. The height was set to the stand-off distance (SOD) of 50 mm. SOD in this test is defined from the face of the target plate to the ground surface.

Fig. 7. Steel pot for the placement of the explosive charge

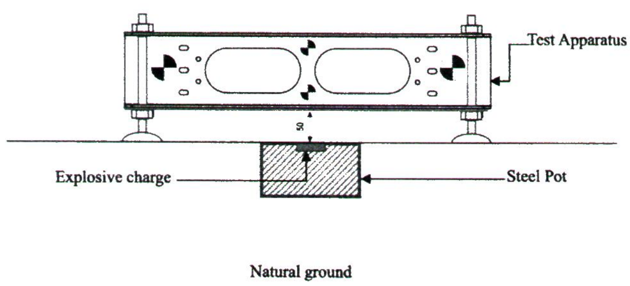

Fig. 8. Setup for Steel Pot testing condition

For both test conditions, an ultra-high-speed video camera was used to observe the global response of the test apparatus (optical observation). It is set up to shoot at 30000 fps and positioned at 0.3 m from the ground level, approximately 5.0 m from the test apparatus. An aluminium box containing synthetic clay was used to gauge the local effect or the peak deflection of the steel plate.

5. Results and Analysis

5.1 Global Blast Impact Variation

Optical observations were performed on both test setups to measure global blast impact. The measurement was based on the test apparatus's response to the blast, which includes the period from when it was elevated vertically to its highest point. Figure 9 shows the test jig's height-time history based on visual observation from the ultra-high-speed video camera.

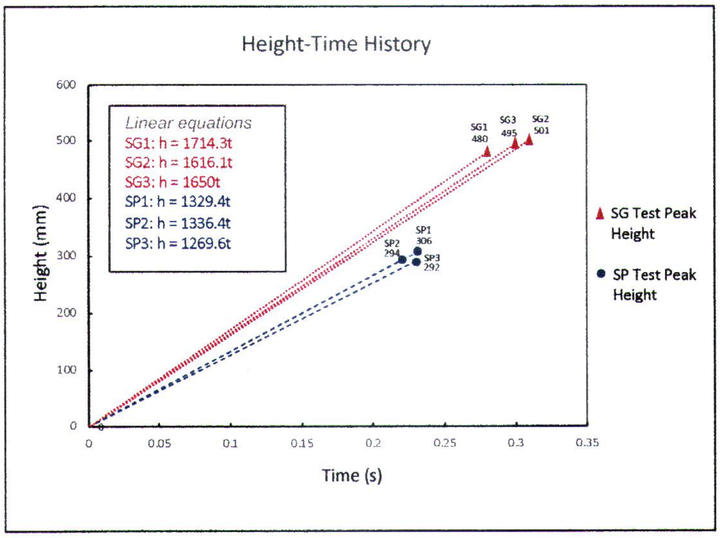

Fig. 9. Linear height-time history of the test apparatus vertical translation to its peak height in the SP and SG tests

Observation during the experimental test appeared to have shown that the test apparatus in the SG testing condition was being uplifted vertically higher compared to the tests in the SP testing condition. On average, the height in SG tests reached up to 492 mm, while the average height in SP was about 297 mm. The peak height would explain the intensity of impact received on the underside of the test apparatus. Converting the blast impact that caused the apparatus to its peak height carrying its self-weight would relate to the total global energy transfer.

A comparison of the global energy transfer in SP and SG tests is shown in Figure 10. The conversion recorded that the average global energy transfer in the SG test is about 40% higher than in the SP test. In the SG test, the average energy transfer is about 117 J compared to the SP test, which is only about 70 J. Higher energy transfer could possibly be caused by the funnelling effect of a crater forming during the detonation phase in soil. When the explosive charge was detonated in the SG test, apart from the energy being absorbed to the ground, the build-up of the reflected tensile wave in the crater [23] was transmitted upwards to the underside of the apparatus. However, in the detonation in the SP test, the detonation did not create a crater. The blast energy, apart from being transmitted upwards, is also dispersed sideways, resulting in less energy transferred to the test apparatus.

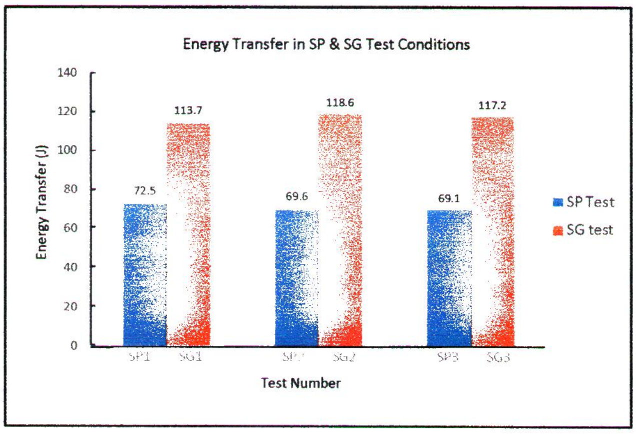

Fig. 10. Global energy transfer in both SP and SG test conditions as a result of blast loads impacting the underside of the test apparatus.

As the test apparatus received the blast impact and was uplifted, it also accelerated in the vertical direction. The global acceleration is obtained from the equation of the linear height-time history path. The peak global acceleration possible time of occurrence was determined within the range of 10 milliseconds to 20 milliseconds, and this is based on previous work by Hassan *et al.,* [8]. By integrating twice, the height-time history linear equation, peak global acceleration is plotted as shown in Figure 11.

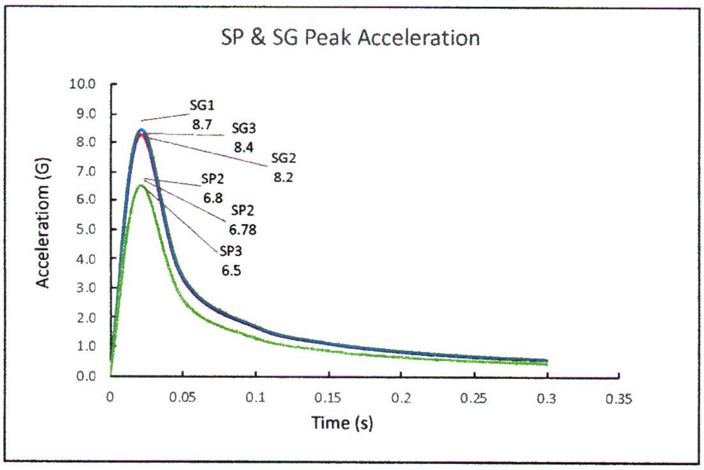

Fig. 11. Global acceleration-time history in tests carried out in SP and SG test conditions.

The peak global acceleration in the SG tests also displayed on a higher side compared to the SP tests. The SG tests recorded peak acceleration as high as 8.7G, while in the SP tests, the highest recorded peak acceleration was 6.8G. Average peak global acceleration for SG and SP tests are about 8.4G and 6.7G, respectively. This is about a 21% difference in the peak acceleration magnitude.

5.2 Local Blast Impact Variation

The local blast effect was measured by observing the peak and residual deformation of the steel target plate. The deformation of the steel plate is affected by both the response of the test apparatus and the direct impact of the blast load on the steel plate. The peak deflection was measured from the shape of the deformed synthetic clay, and the residual deflection was measured from the shape of the deformed steel plate. The post-blast test profiles in the Steel Pot and Sandy Gravel test conditions where the residual and peak deflection of the steel plate were plotted are shown in Figure 12.

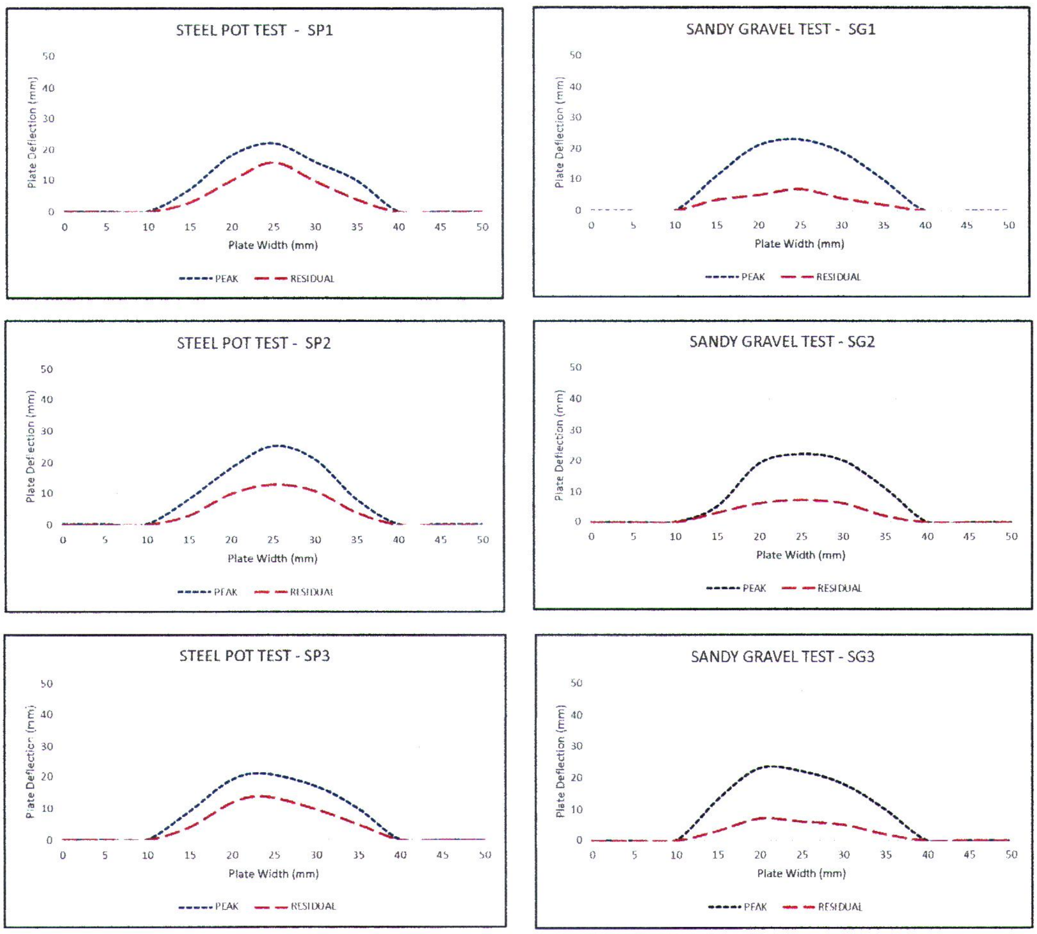

Fig. 12. Post blast test profiles in the Steel Pot and Sandy Gravel test conditions which shows the residual and peak deflection of the steel plate

Generally, from the plotted deformation profiles of the steel plates, the steel plates experienced almost similar levels of peak deflection. However, the residual deflection in the SP test condition is more prominent. The average peak deflection in the SP test condition is about 24.7 mm, and in the SG test condition, the average peak deflection acquired is about 22.7 mm. The peak deflection varies by about 8%, where it is higher in the SP test condition. For the residual deflection, which is the observable post-blast test steel plate deflection, the average deflection is 13.7 mm in the SP test and 7 mm in the SG test condition. This is almost a 5% variation in residual deflection where the SP test experienced on the higher side. Tables 1 and 2 show the tabulation of the local deflection that occurred on the steel plate for the SP and SG tests, respectively.

Table 1
Local effects of the steel plate in Steel Pot testing condition

Steel Pot Testing Condition			
Test	*Residual Deformation (mm)*	*Peak Deformation (mm)*	*Plate Peak Acceleration (G)*
SP1	14	25	16000
SP2	13	25	16000
SP3	14	24	15300

Table 2
Local effects of the steel plate in Sandy Gravel testing condition

Sandy Gravel Testing Condition			
Test	*Residual Deformation (mm)*	*Peak Deformation (mm)*	*Plate Peak Acceleration (G)*
SG1	7	23	14700
SG2	7	22	14000
SG3	7	23	14700

The steel plate peak acceleration, as in Tables 1 and 2, was obtained through double integration of the peak deflection with time. The time of occurrence of steel plate peak deflection was determined at 0.4 milliseconds based on the reading recorded by a piezoelectric shock accelerometer from previous work [18]. The average plate peak acceleration derived in the SG test is about 14500 G, compared to the SP test condition, which is almost 15800 G. A variation of 8.2% in terms of localised acceleration.

Looking at the results of local effects, the local plate deformations and peak acceleration in the SG test are lower than in the SP test. This contradicts the results obtained for global average energy transfer and average acceleration, where the SG test results are higher than the SP test results. In the localised blast effect, the close stand-off distance is considered as within the fireball of the explosion. For the SP tests where the explosive charge is detonated in the steel pot, the blast loading hits directly towards the target steel plate, and the rigid base of the steel pot further amplifies the impact. As a result, the reflected blast wave causes a higher plate deformation and acceleration.

In the SG test, the detonation blast waves are not fully reflected. Blast waves are transmitted to their surroundings, including to the ground, in the form of ground shock and create a crater within the rupture zone. This reduces the initial local impact intensity on the steel plate, which is crucial in causing deformation. However, the crater contributes to the funnelling effect that intensifies the global impact in uplifting the test apparatus. The intensity of funnelling effects depends on the characteristics of the crater attributed to the soil properties.

6. Conclusions

From the testing conducted in this experiment, conflicting variations appear in the testing conditions described in STANAG 4569-AEP55. In the Steel Pot test condition, the effects of local impact are higher than in the Sandy Gravel test condition. However, the effects of global impact are higher in the Sandy Gravel test condition compared to the Steel Pot test condition. For the local impact, the steel plate residual and peak deflection are higher by 5% and 8%, respectively, in the Steel Pot test condition. This is exhibited by the steel plate peak acceleration, which is 8.2% higher than the Sandy Gravel test condition.

The effect of total reflected detonation blast wave contributes to higher local impact in the Steel Pot test. Nevertheless, global energy transfer is 40% higher in the Sandy Gravel test, and the peak acceleration is also 21% higher compared to the Steel Pot test. Funnelling effects in the Sandy Gravel test from the crater that formed during the detonation contribute to higher global impact. The variations in blast effects show that the testing conditions, as described in the STANAG 4569-AEP55, should be opted for based on a specific vehicle's protection requirements.

Acknowledgement
This research was funded by a grant from the National Defence University of Malaysia (Short Term Grant UPNM/2022/GPJP/TK/7).

References

[1] Mildef. (n.d.). Mildef International Technologies. Retrieved June 2023, from http://mildef.com.my/portfolio-item/hmav/
[2] NATO. (2012). STANAG 4569 (Ed. 2) -Protection levels for occupants of armoured vehicles. NATO Standardization Agency .
[3] Robert, W., Ceh, M., & Josey, T. (2016). Characterization of buried landmine blast. . Suffield: Defence Research and Development Canada.
[4] Clarke, S. D., Fay, S. D., Tyas, A., Warren, J., Rigby, S., Elgy, I., & Liversey, R. (2014). Repeatability of buried charge testing. Proceedings of the 23rd International Symposium on Military Aspects of Blast and Shock. Oxford, UK.
[5] Clarke, S. D., Fay, S. D., Warren, J. A., Tyas, A., Rigby, S. A., Reay, J. J., . . . Elgy, I. (2017). Predicting the role of geotechnical parameters on the output from shallow buried explosives. International Journal of Impact Engineering, 102, 117-128. https://doi.org/10.1016/j.ijimpeng.2016.12.006
[6] Hassan, Z. A., Ibrahim, A., & Nor, N. M. (2019). Effect of Crater's Shape and Profile on Blast Wave Transfer of Shallow Buried Charge Detonation. Proceedings of the 32nd International Symposium on Shock Waves (ISSW32 2019). Singapore. https://doi.org/10.3850/978-981-11-2730-4_0407-cd
[7] Hassan, Z. A., Ibrahim, A., & Nor, N. M. (2019). Feasibility of a small-scale test apparatus in measuring blast intensity of shallow buried charge detonation in in-situ soil. Science and Technology of Energetic Materials, 80(6), 229-236.
[8] Hassan, Z. A., Ibrahim, A., & Nor, N. M. (2020). Optical observation of detonation of shallow buried charge in sandy soil. Defence S and T Technical Bulletin, 13(2), 255-266.
[9] Hlady, S. L. (2004). Effect of soil parameters on land mine blast. 18th Int. Sym. on Military Aspects of Blast and Shock (MABS18). Bad Reichenhall, Germany.
[10] Clarke, S. D., Fay, S. D., Warren, J. A., Tyas, A., Rigby, S. E., Reay, J. J., & Liversey, R. (2015). Geotechnical causes for variation in output measured from shallow buried charges. International Journal of Impact Engineering, 274-283.
[11] Taylor, L. C., Skaggs, R. R., & Gault, W. (2005). Vertical impulse measurement of mines buried in saturated sand. International Journal for Blasting and Fragmentation, Fragblast, 9, 19-28.
[12] Ehrgott, J. Q., Akers, S. A., Windham, J. E., Rickman, D. D., & Danielson, K. T. (2011). The influence of soil parameters on the impulse and airblast overpressure loading above surface-laid and shallow-buried explosives. Shock and Vibration 18, 857-874.
[13] Tremblay, J. E., Bergeron, D. M., & Gonzalez , R. (1998). Key technical activity 1-29: protection of soft-skinned vehicle occupants from landmine effects. In Technical cooperation program. Val-Belair, Canada: Defence Research Establishment Valcartier.
[14] Deshpande, V. S., McMeeking, R. M., Wadley, H. N., & Evans, A. G. (2009). Constitutive model for predicting dynamic interactions between soil ejecta and structural panels. Journal of the Mechanics and Physics of Solids 57, 1139-1164.
[15] Bergeron, D., Walker, R., & Coffey, C. (1998). Detonation of 100-gram anti-personnel mine surrogate charges in sand: A test case for computer code validation. Technical Report 668. Ralston, Alberta, Canada: Defence Research Establishment Suffield.

[16] Ambrosini, D., Luccioni, B., & Danesi, R. (2003). Craters produced by explosions on the soil surface. Mecanica Computacional Vol. XXII, (pp. 678-692). Bahia Blanca, Argentina.
[17] Rigby, S. E., Fay, S. D., Tyas, A., Clarke, S. D., Reay, J. J., Warren, J. A., . . . Elgy, I. (2018). Influence of particle size distribution on the blast pressure profile from explosives buried in saturated soils. Shock Waves, 28(3), 613-626.
[18] Hassan, Z. A., Ibrahim, A., & Nor, N. M. (2018). Small-scale experimental test on the effect of in-situ tropical soil on shallow buried charge blast intensity. Military Aspects of Blast and shock MABS25. The Hague, The Netherlands.
[19] Fay, S. D., Clarke, S. D., Tyas, A., Warren, J., Rigby, S. E., Bennett, T., . . . Gant, M. (2014). Measuring the spatial and temporal pressure variation from buried charges. Proceedings of the 23rd Intl. Symp. of Military Aspects of Blast and Shock. Oxford.
[20] Fourney, W. L., Leiste, U., Bonenberger, R., & Goodings, D. J. (2005). Mechanism of loading on plates due to explosive detonation. Fragblast, 9(4), 205-217.
[21] Linforth, S., Tran, P., Rupasinghe, M., Nguyen, N., Ngo, T., Saleh, M., . . . Shanmugam, D. (2019). Unsaturated Soil Blast: Flying Plate Experiment and Numerical Investigations. International Journal of Impact Engineering, 125, 212-228.
[22] Bouamoul, A., Gourdeau, F. F., Toussaint, G., & Durocher, R. (2014). An empirical model for mine-blast loading. Defence R&D Canada, Valcartier Research Centre.
[23] Ramasamy, A., Hill, A. M., Hepper, A. E., Bull, A. M., & Clasper, J. C. (2009). Blast Mines: Physics, Injury Mechanisms and Vehicle Protection. Journal of Royal Army Medical Corps 155(4), 58-264.